

Land Cover Classification Using Band Ratioing for Higher Accuracy in Hilly Terrain of Mandakini Valley, Central Himalaya.

Suman Das¹, Suraj Prasad², Lungaithui Kamei³

¹Department of Geography, Kirori Mal College, University of Delhi, Delhi – 110007

²Department of Geography, Central University of Jharkhand, Ranchi – 835222

³Department of Geography, Shaheed Bhagat Singh Evening College, University of Delhi, Delhi – 110017

Received: 16.07.2024

Revised: 19.08.2024

Accepted: 22.09.2024

Abstract

This paper describes Remote Sensing as an advanced Space Technology for Land use land cover (LULC) classification with particular emphasis on Image Statistic for the rugged terrain of the central Himalaya. Digital image classification is widely used to produce land cover maps from remote sensing data at present. The performance of image classification that utilizes only the remote sensing data often deteriorates, due to the presence of shadows of high peaks, especially in mountainous regions. In this study, a multi-source image classification approach has been used to map land cover in the Himalayan region of Rudraprayag District with high mountain peaks having elevations up to 6654 m above mean sea level has. Remote sensing data from IRS LISS IV image along with Normalized Difference Vegetation Index (NDVI) and Digital Elevation Model (DEM) data layers were used to perform multi-source image classification using supervised maximum likelihood classifier method. The results exhibit a notable improvement in the accuracy of classification from 71.25% to 89.33% on integrating of NDVI and DEM as ancillary data with the spectral data of satellite image.

Key Word: Land Use Land Cover, Maximum Likelihood Classifier, LISS IV, NDVI, DEM.

1. Introduction

Land use Land cover classification is the process of grouping pixels into a finite number of individual classes based on their pixel values. If a pixel fulfils a specific set of criteria, then the pixel is assigned to the particular class that corresponds to that criteria. This process is also known to as image segmentation. The knowledge of spatial land cover information is essential for proper management, planning and monitoring of natural resources (Zhu, 1997). Remote sensing image for LULC classification has proven to be useful for extracting useful thematic information such as land cover mapping in mountainous regions such as the Himalaya since these areas are generally inaccessible due to high altitudes and ruggedness of the terrain (Saha et. Al., 2005). In past years, several studies to map LULC using remote sensing data in high hilly areas have resulted with different level of accuracy which may be governed by a large number of factors that affect the remote sensing process. Those as mentioned earlier may be due to the presence of hill shadows owing to the high elevation of the terrain, deep valleys, the cloud cover, steep slopes low sun angles, and differential in canopy cover. Therefore, due to changes in environmental conditions, spectral characteristics also change from one region to the other (Arora and Mathur, 2001; Saha et. Al., 2005).

Hence, classification only based on spectral data from a remote sensing sensor alone may not be sufficient to gather useful land cover information. Incorporation of additional or ancillary data sources in the process of remote sensing classification may result in better understanding and achievement of higher accuracy than utilizing spectral data from a remote sensing sensor alone (Watanachaturaporn et al., 2008). The ancillary data from various sources may be available in different forms and contexts, and at different frequencies, time, and spatial domains. Integration of data from different sources may also be referred to as image data fusion (Pohl and van Genderen, 1998). Depending on the nature of data sources and methodology used, image fusion may be categorized as multi-source, multi-sensor, multi-temporal, multi-frequency, multi-polarization, or multi-resolution fusion (Arora and Mathur, 2001; Rao and Arora, 2004; Simone et al., 2002). The classification of remote sensing data along with data from other sources, has generally been referred to as multi-source classification. In the past, several studies (e.g., Benediktsson and Sveinsson, 2003; Bruzzone et al., 1999; Fitzgerald and Lees, 1994; Peddle et al., 1994) were conducted on multi-source classification, and significant improvement in classification accuracy was achieved. Moreover, a number of derivatives of multispectral images such as Normalized Difference Vegetation Index (NDVI) and Digital Elevation Model (DEM) may also be incorporated in the classification process to enhance the quality of land cover classification from remote sensing data in mountainous regions (Eiumnroh and Shrestha, 2000; Saha et al., 2005).

This study aims to present a case study to derive accurate land cover map using the multispectral image from IRS-LISS-IV sensor as the primary data with NDVI and DEM as the additional data layers to implement multi-source land cover classification using the logical channel approach (Tso and Mather, 2001) on a recent disaster-affected area with high elevation and rugged terrain of Mandakini Valley in the Himalayas. The Separability analysis also measures based on transformed divergence value to examine the relative importance of various spectral bands and ancillary data layers in the classification process. Most widely used Maximum Likelihood Classifier (MLC) has been used to perform the classification.

2. Study Area

The Mandakini watershed (Figure 1) in the Garhwal Himalaya is located at the western end of the Central Himalaya. The catchment stretches from Kedarnath in the north to Rudraprayag in the south, from 30°15'N to 30°45'N and 78°45'E to 79°30'E falling in Survey of India Toposheet Nos. 53J and 53N. The total area of the Mandakini valley for which a LULC map has been prepared is 1563 km². Mandakini River is the main stream originating from the Chorabari Glacier at an elevation of 3840m and joining the Saraswati River (which originates from the Companion glacier) at Kedarnath. The Mandakini River joins the Alaknanda River at Rudraprayag. The major tributaries of the Mandakini River are the Madhmaheshwar, Kali and Son Rivers. The Mandakini River crosses the Main Central Thrust (MCT) that separates the Higher Himalaya from the Lesser Himalaya. The MCT zone is composed of many faults with fractured and weathered rocks. The main roadway in the watershed connects Rudraprayag in the south to Sonprayag in the north. Beyond Sonprayag, people trek about 17 km to reach Kedarnath town where the famous Kedarnath Temple is located (Naithani et al., 2011; Sati et al., 2011; Singh et al., 2014). Other roads connect significant towns and villages in the catchment. Many slopes along the roads have become unstable due to widening of roads in recent Chardham project as well as new construction of road under Pradhan Mantri Gramin Sarak Yojana and poorly designed undercutting of hillslopes to support high-volume traffic during the pilgrimage season.

Moreover, the physical setting in the catchment has created many unstable steep slopes with loose material that are susceptible to failure in response to various triggers, including earthquakes and high-intensity rainfall during the monsoon season, which accounts for 50–

90% of total annual rainfall (Asthana and Sah, 2007; Larsen and Montgomery, 2012; Khandelwal et al., 2015). The climate of the study area is humid-temperate in summer and dry, humid cold in winter. The climate of the area is subtropical at high elevations (mean annual rainfall is 100–150 cm) to humid subtropical at a lower altitude (150 to 200 cm yearly rainfall) with 80% of the rain occurring in the monsoon period from mid-June to mid-September.

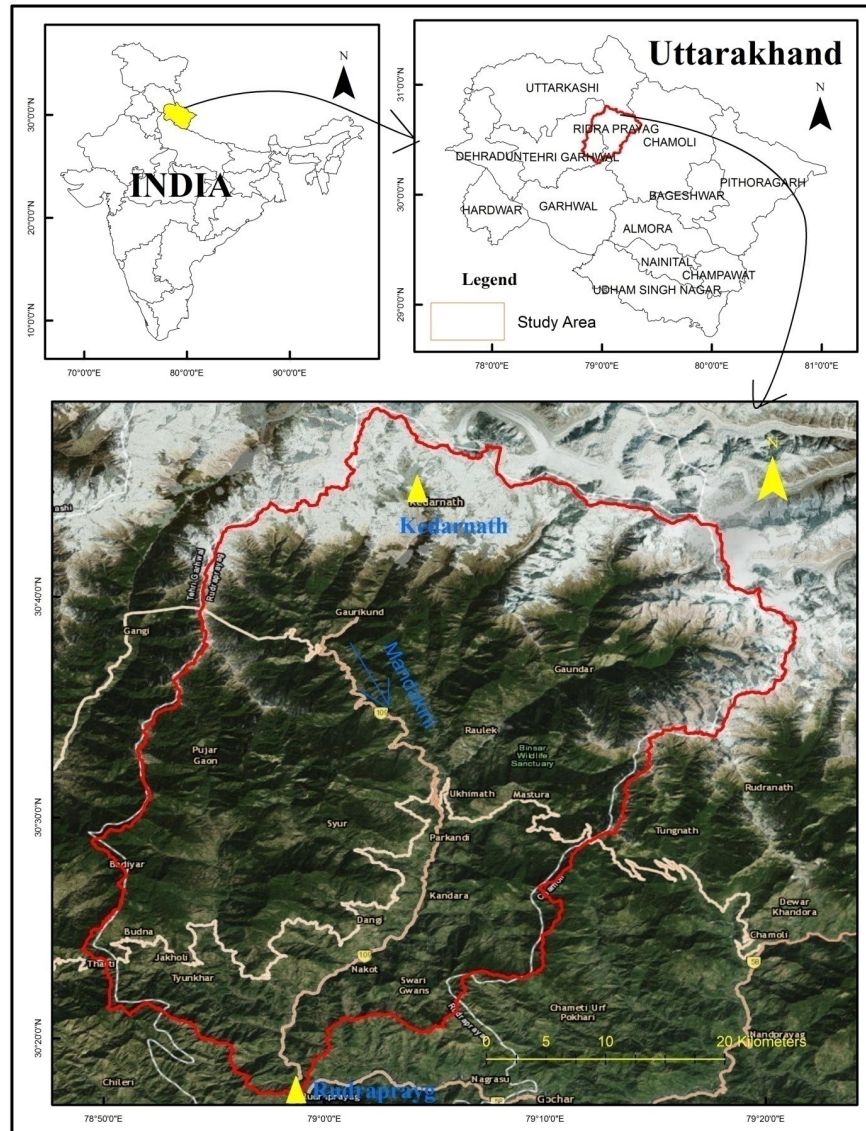


Figure1: Study Area, Mandakini Watershed

3. Data Used:

The present study is based on mapping land cover from IRS-1D, LISS-IV remote sensing data. The LISS IV multispectral image with 5 m spatial resolution (Fig. 2a) has been used as the primary data for LULC classification, whereas the Google Earth image and Toposheets has been used as reference data for the creation of training and testing data sets. Additional or

ancillary data namely DEM from Cartosat 1 and NDVI extracted from the LISS-IV image also incorporate in the process of remote sensing classification for better result and achievement of higher accuracy than using spectral data from a remote sensing sensor alone. More description of these data sets is provided in Table 1.

The preparation of referenced data was ably assisted with field surveys conducted in December 2015, which show for same atmospheric and environmental conditions over the area. Due to the inadequate road networked and thus inaccessible due to high elevations and ruggedness, the information on existing land cover was collected only along the accessible roads during the field surveys.

Table 1: Remote sensing and other data Characteristics used in the study.

Data Type	Data Sources	Date of Acquisition
IRS 1D LISS IV image in 3 bands (Green: 0.52 - 0.59 μ m, Red: 0.62 - 0.68 μ m and NIR: 0.77 - 0.86 μ m)	National Remote Sensing Agency (NRSA), India	6 th December 2012
Digital elevation model (DEM) Cartosat-1 PAN(2.5m) Stereo Data V3R1:2014	National Remote Sensing Agency (NRSA), India	29 th April 2014.
Topographic maps (Sheet Number H44G/6,14,15,16; H44H/1,2,3,4,6,8,14; H44I/3,4,8; H44M/13; H44N/1,5; scale 1:50,000)	Survey of India,	During 1962-63
Field data on land use/land cover	Ground truth collected during the study	December, 2015.

4. Methodology:

Plenty of data processing steps are involved in performing multi-source classification. These include image mosaic, subset to Aoi, generation of ancillary data layers, image classification and accuracy assessment. All the processing has been done on Arc GIS, and ERDAS Imagine software. DEM and NDVI data layers were used as additional bands (referred to as ancillary data) to perform multi-source classification. The processing steps are briefly described below.

4.1 Pre-processing of satellite image

The DEM data of Cartosat 1 satellite was downloaded from NRSC Bhuvan. The Elevation mosaic and boundary of Mandakini watershed extracted by using the command of Arc-GIS. The Cartosat 1 DEM then resampled to 5m as of LISS IV image. Similar way, the spectral data of LISS IV satellite were stacked and mosaic. Therefore, the watershed boundary generated from DEM has used for subset the spectral imageries. Along with the spectral data incorporation of two additional bands, namely NDVI and DEM, also were stacked to enhance the quality of classification. So, the dataset for multi-source classification consisted of five data layers (three bands of multispectral LISS IV image, two ancillary data sources - NDVI and the DEM). For convenience, Green band, Red band, NIR band, NDVI and DEM data layers have been numbered as 1, 2, 3, 4, and 5 sequentially.

4.2 Generation of Ancillary Data

The incorporation of additional bands, namely NDVI and DEM, were used in the classification process to enhance the quality of land cover classification and achieve higher accuracy in mountainous regions.

4.2.1 Generation of DEM

The DEM data of Cartosat 1 satellite (figure 2b) was used as ancillary data in the classification process. In hilly areas, a major variation in the brightness values of pixels can be found due to the presence of shadows, which may lead to misclassification of the image. Therefore, the DEM was used as ancillary data in the classification process to reduce some confusion between shadowed areas and water bodies (Yocuaba, et. Al., 2010). Moreover, the elevation information from DEM may also act as a logical rule to eliminate the presence or absence of certain classes in particular elevation zones. For example, fallow land is not expected to exist at higher elevations that are covered with snow since climatic conditions do not allow for any agricultural activity at such high elevations. Thus, these areas should be categorized as barren land. Therefore, any presence of fallow land in the neighborhood of snow-covered areas may represent a misclassification, which can be reduced by including a DEM in the remote sensing classification process (Saha. et. Al., 2005).

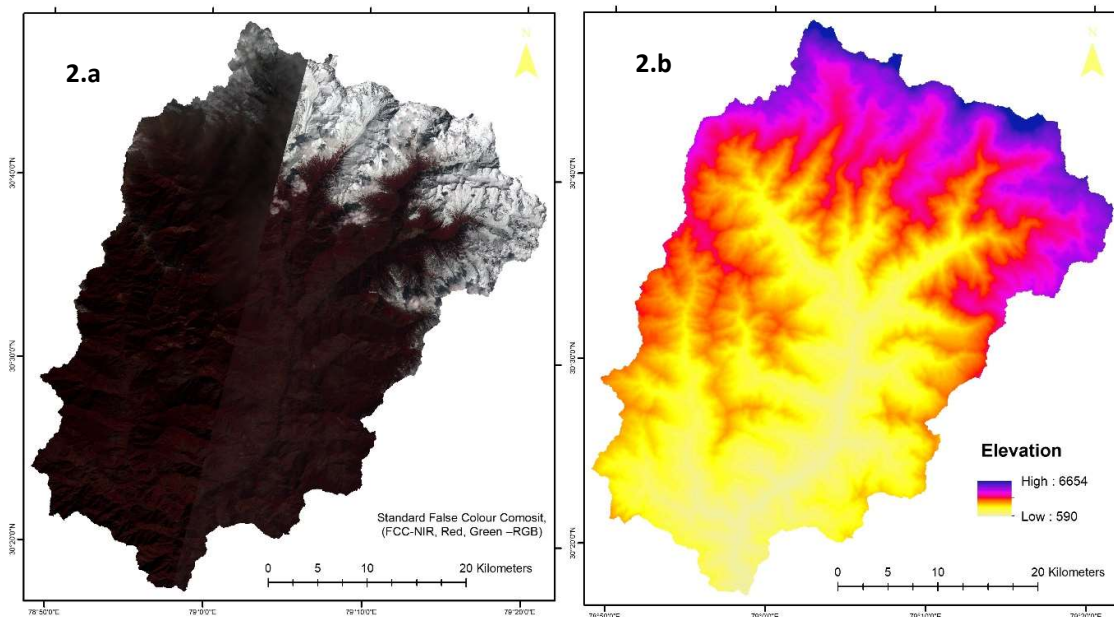


Figure 2: IRS 1D LISS IV colour infrared composite, NIR, Red, Green -RGB, (2.a) & IRS Cartosat DEM stereo Data (2.b).

4.2.2 Generation of NDVI

NDVI was used as another ancillary data layer in the classification process to enhance the separability of the spectral band among various land use classes and also to reduce the shadow effect due to variations in topography. The NDVI data layer was generated from NIR and Red bands of LiSS IV image and is defined as:

$$NDVI = \frac{(NIR - R)}{(NIR + R)} \quad (1)$$

Whereas NIR represents the spectral reflectance in a near-infrared band while R represents the red band. The negative values and value near zero indicate non-vegetation classes, such as snow, water, barren land, built-up areas, whereas positive values represent different types of vegetation classes (Fig. 3). The NDVI values vary from -0.20 to +0.73.

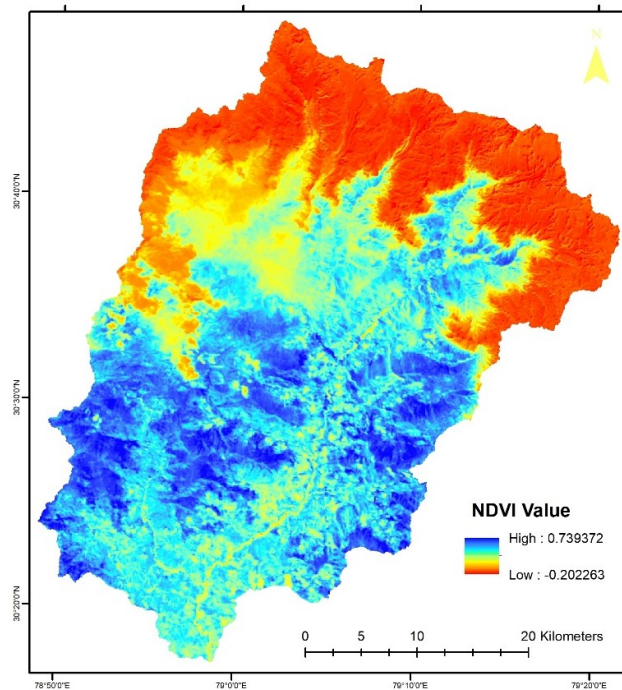


Figure 3: NDVI from IRS 1D LISS IV image

4.3 Image Classification

In this study supervised classification of Maximum Likelihood classifier has been used in Erdas Imagine platform. Supervised classification methods are most commonly used in remote sensing and based on the knowledge of the area to be classified. "These methods are often central to the image analysis process since these concerns the direct transformation from pixel counts to thematic map" (Wilkinson, 2000). Supervised classification may be defined as the process of identifying unknown objects by using the spectral information derived from training data provided by the analyst. The result of the identification is the assignment of unknown pixels to pre-defined categories.

Table 2: Characteristics of land cover classes

LULC Class	Description	Characteristics on LISS-IV FCC
Snow	Snow-covered areas on high altitude mountains	Bright white
Water Body	Rivers and lakes	Cyanish blue to blue depend on sediment content and depth of the water
Dense Vegetation	Tall, dense trees	Dark red with rough texture

LULC Class	Description	Characteristics on LISS-IV FCC
Sparse Vegetation	Low vegetation density with an exposed ground surface	Dull red to pinkish with a smooth texture
Agricultural Land	Crops on hill terraces as step cultivation	Dull red and step-like arrangement
Fallow Land	Agricultural fields without crops	Bluish/greenish grey with smooth texture
Barren Land	Exposed rocks without vegetation	Yellowish with a bright tone
Fresh Sediment	Fresh landslide debris and river sediments on the bank	Cyanish in a bright tone
Settlement	Towns and villages; block-like appearance	Bluish with a blocky appearance

Maximum Likelihood Classifier has been found to be the most accurate and commonly used classifier when distributional data assumptions are met. This classifier is based on the decision rule that the pixels of unknown class membership are allocated to those classes with which they have the highest likelihood of association (Foody et al., 1992). It requires estimates of the mean vector and variance-covariance matrix for each class. In this study, MLC has been used here to produce a nine of land cover classes using different band combinations based on previous studies done over the Himalayan region with magnificent mountain peaks with elevations up to 4785 m above mean sea level (Saha et al. 2005). The particular description of these classes along with their interpretative characteristics on the False Colour Composite (FCC) of LISS-IV image is provided in Table 2.

4.4 Preparation of training dataset

The volume of the training data set is also significant in supervised classification if statistical estimates are to be reliable. As the success of a classification highly depends on the quality of the training data, these must be selected from the representative of the region of the land cover classes under investigation. Data should thus be collected from relatively homogeneous areas consisting of those classes. The sample size is mainly related to the number of features whose statistical properties are to be estimated. Typically, it is recommended that the minimum training set size is some 10-30 times the number of wavebands per class being used for classification (Mather, 1999; Piper, 1992). Generally, an extensive training set is required for mapping from multispectral datasets. Supervised classification methods require more user interaction, especially in the collection of training data. In this study, the training data set consisted of about 1.23% of the total pixels in the LISS IV image. The number of training samples for each LULC class (Table 3) were chosen in proportion to the area covered by the respective classes on the ground. The High spatial resolution Google Earth image and topographic map were used as reference data (ground truth) to delineate the training pixels on the LISS IV image. Wherever there appeared to be confusion in identifying the classes, these were verified in the Google Earth Image or in toposheet and if accessed then in the field. The quality of training data of each class evaluated through histogram plots. Most of the training pixel in each class were typically distributed having a single peak, which is a necessity of the maximum likelihood classifier used in this study.

Table 3: Number of training pixels for each land cover class used in classification

LULC Class	Number of Training Pixels
Snow	317546

LULC Class	Number of Training Pixels
Water Body	1812
Dense Vegetation	329128
Sparse Vegetation	76015
Agricultural Land	53502
Fallow Land	8924
Barren Land	10772
Fresh Sediment	11631
Settlement	4176
Total	813506

4.5 Separability analysis

The dataset for multi-source classification consisted of five data layers (three bands of multispectral LISS IV image, two ancillary data sources - NDVI and the DEM). For convenience, Green band, Red band, NIR band, NDVI and DEM data layers have been numbered as 1, 2, 3, 4, and 5 respectively. A separability analysis was performed using the training dataset, selected earlier, to identify the combination of bands that shows the highest distinction between the land cover classes. Separability is a statistical measure devised based on spectral distances computed for a combination of bands. From several separability measures, the Transformed Divergence (TD) has been used in this study (Jensen, 1986). The TD values range from 0 to 2000. A value close to 2000 indicates the best separability. The values between 1800 and 2000 are generally considered adequate for the selection of appropriate band combinations. Since, the aim of the present study is on the inclusion of ancillary data in the classification process, the average TD values of various band combinations that included ancillary data, was computed.

Various band combinations that produced average TD values near to 2000 were considered appropriate for classification (Table 4). The band combination 1, 2, 3, 4 and 5 resulted in the highest average TD value, which illustrates that LISS IV image together with DEM and NDVI data layer, has produced the best separability among various pairs of land cover classes.

Table 4: Various band combinations and their average TD values

**Band Combination	Average TD
1,2,3	1691
1,2,3,4	1991
1,2,3,5	1983
1,2,3,4,5	1992

** (Bands 1,2,3: LISS IV bands; Band 4: NDVI; Band 5: DEM)

4.6 Accuracy assessment

Accuracy assessment is essential for image classification, especially when the classification data is to be used for change detection. To evaluate the accuracy of the classified image, a random sample of the testing pixel is selected on the classified image, and then their class is

compared with the reference data or ground-truthing. The choice of a suitable sampling scheme and the determination of an appropriate sample size for testing data plays a vital role in the assessment of classification accuracy (Arora and Agarwal, 2002).

In the accuracy assessment process, the overall accuracy indicates the accuracy of the complete image classification. It is a probability that the number of precisely classified pixels divided by the whole number of pixels in the error matrix). In contrast, users and producers accuracy measures indicate the accuracy of individual classes. Users accuracy is defined as the probability that a pixel classified on the map actually represents that class on the real world or reference data. In contrast, producer's accuracy establishes the possibility that a pixel on reference data has been classified correctly. In this study, information from Google earth Image, together with Toposheet and field visits, was used as reference data to generate testing data set. Stratified random sampling method was applied for the generation of the testing pixel. A total of 150 testing pixels for each class were selected, which are significantly larger than the sample size of 75 to 100 pixels per class, as recommended by Congalton (1991) for accuracy assessment purposes. For a valid comparison, the same testing dataset was used to determine the overall and producer's accuracy for LULC classes from the classified images of different band combination.

Table 5: Producer's accuracy of individual classes derived from classifications using band combination 1,2,3 & 1,2,3,4,5

Classes	Producer Accuracy (in %)	
	Band 1,2,3	Band 1,2,3,4,5
Snow	82.00	93.75
Water Body	75.33	84.00
Dense Vegetation	77.00	91.67
Sparse Vegetation	79.50	88.56
Agricultural Land	72.50	91.50
Fallow Land	66.67	78.67
Barren Land	74.29	90.50
Fresh Sediment	75.00	71.00
Settlement	68.44	86.67
Overall Accuracy	85.21	91.04

5. Results and Discussions

The objective of this study is to execute a multi-source classification approach to produce an accurate land cover map for the rugged terrain of Himalaya. The accuracy of land cover maps obtained from multi-source classification of a dataset using band combinations 1,2,3,4,5 is highest as of 91.04% while classification based only on spectral data of LISS IV image using band combination 1,2,3 produced an accuracy of 85.21%. So, on the inclusion of NDVI and DEM data layer with spectral data accuracy in the classification process increased remarkably. To assess the classification accuracy of individual land cover classes, producer's accuracies were also determined for the classification that provided the highest overall accuracy (i.e., the classification obtained by using band combination 1, 2, 3, 4, 5). These accuracy values were also compared with those obtained from the classification produced by using only LISS IV satellite spectral data (Table 5). A glance at producer's accuracy values shows that the accuracy of most of the classes has increased when NDVI and DEM data layers added in the classification process. So it is illustrated that the misclassifications

between the classes have been reduced. In particular, the classes, namely Waterbody, snow, sparse vegetation, agriculture, fallow and barren land and settlements, showed a substantial increase in accuracy ranging from 5% to 15%. The reason behind the increase in accuracy is that the barren land class was considerably misclassified with the class settlements when only spectral data were used. Since, at high elevations, the presence of these classes is scarce, the addition of DEM data layer reduced this misclassification. Secondly, due to the presence of shadows in the region, the classification using only spectral data showed misclassification of agriculture and fallow land to the class sparse vegetation. The addition of NDVI and DEM data layers reduced the shadow effect and resulted in the reduced this misclassification.

On visual comparison of two classified images using only spectral band 1,2,3 (Fig. 4a) with FCC and using band combination 1,2,3,4,5 (Fig. 4b), it is observed that the addition of DEM and NDVI ancillary data layers resulted in the correct classification of shadowed areas to their corresponding vegetation classes, which was not the case when only spectral data was used for classification. Thus, this study clearly demonstrates the utility of incorporating NDVI and DEM in the image classification process, especially for rugged terrain.

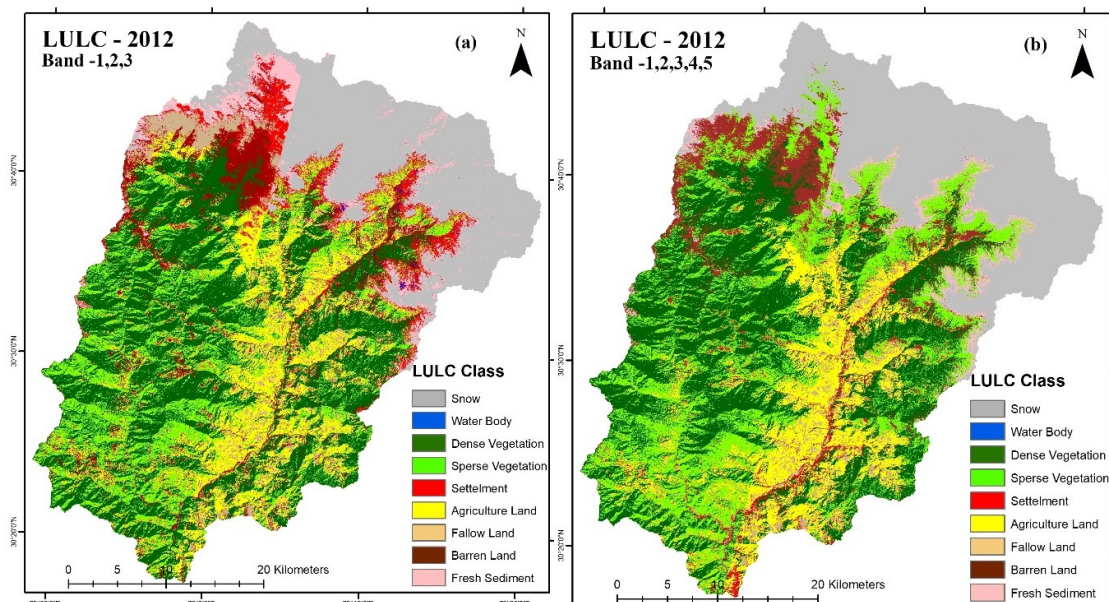


Figure 4: The LULC classification produced from the band combination 1, 2, 3 (fig.4.a) and created from the band combination 1, 2, 3,4,5 (fig.4.b) (i.e., Green, Red and INR bands of IRS LISS IV image, NDVI image and DEM)

6. Conclusions

Remote sensing data are attractive for land use land cover classification, especially for the hilly region where most of the area is inaccessible due to ruggedness in topography and high altitudes of the terrain. However, remote sensing data acquired over a mountainous region with high relief resulted in shadowed regions which lead to inaccurate classification if only spectral data from remote sensing sensors were used. Therefore, ancillary data were included to enhance the quality of image classification. The case study presented in this paper also showed a remarkable increase in accuracy of land cover classification on the incorporation of NDVI and DEM data layers with IRS-LISS-IV image. The classification

produced from remote sensing data alone, it was revealed that the class dense forest, sparse vegetation, fallow land, and barren land are highly confused with other classes resulting in misclassifications and thus lowering the accuracy. However, these misclassifications were reduced on the addition of NDVI data and were further reduced when the DEM data were included. The classes were mapped with high accuracy when both the NDVI image and the DEM were included, as the misclassifications decreased significantly. The present study thus highlights the effectiveness of integrating DEM and NDVI data layers with the spectral data to enhance the quality of land cover classifications in mountainous regions such as the Himalayas.

Acknowledgments

The author is grateful to Dr. A. K. Saha for his guidance and supervision and to Dr. M. S. Panwar for his assistance during field surveys.

References:

1. Arora, M K and Mathur, S. 2001. Multi-source Classification Using Artificial Neural Network in a Rugged Terrain. *Geocarto International*, 16(3), 37-44.
2. Arora, M K and Agarwal, K. 2002. A program for sampling design for image classification accuracy assessment. *Photogrammetry Journal of Finland*, 18(1), 33-43.
3. Asthana, A.K.L., & Sah, M.P., 2007. Landslides and cloudbursts in the Mandakini Basin of Garhwal Himalaya. *Himal. Geol.* 28 (2), 59–67.
4. Benediktsson, J.A., and J.R. Sveinsson, 2003. Multisource remote sensing data classification based on consensus and pruning, *IEEE Transactions on Geoscience and Remote Sensing*, 41(4):932–936.
5. Bruzzone, L., and D.F. Prieto, 1999. A technique for the selection of kernel function parameters in RBF neural networks for classification of remote sensing images, *IEEE Transactions on Geoscience and Remote Sensing*, 37:1179–1184.
6. Congalton, R G. 1991. A review of assessing the accuracy of classifications of remotely sensed data. *Remote Sensing of Environment*, 37, 35-47.
7. Eiumnoh, A and Shrestha, P. 2000. Application of DEM Data to Landsat Image Classification: Evaluation in a Tropical Wet-Dry Landscape of Thailand. *Photogrammetric Engineering & Remote Sensing*, 66(3), 297-304.
8. Fitzgerald, R.W., and B.G. Lees, 1994. Assessing the classification accuracy of multisource remote sensing data, *Remote Sensing of Environment*, 47(3):362–368.
9. Foody, G M, Campbell, N A, Trodd, N M and Wood, T F. 1992. Derivation and applications of probabilistic measures of class membership from maximum likelihood classification, *Photogrammetric engineering and remote sensing* 58: 1335-1343
10. Khandelwal, D.D., Gupta, A.K., Chauhan, V., 2015. Observations of rainfall in Garhwal Himalaya, India during 2008–2013 and its correlation with TRMM data. *Curr. Sci.* 108 (6), 1146–1151.
11. Larsen, I.J., Montgomery, D.R., 2012. Landslide erosion coupled to tectonics and river incision. *Nat. Geosci.* 5 (7), 468–473.
12. Mather, P. M., 1999, *Computer Processing of Remotely-Sensed Images: An Introduction*. Second Edition, Chichester: John Wiley and Sons.

13. Naithani, A.K., Rawat, G.S., Nawani, P.C., 2011. Investigation of landslide events on 12th July 2007 due to cloudburst in Chamoli district, Uttarakhand, India. *Int. J. Earth Sci. Eng.* 4 (5), 777–786.
14. Peddle, D.R., G.M. Foody, A. Zhang, S.E. Franklin, and E.F. LeDrew, 1994. Multisource image classification II: An empirical comparison of evidential reasoning and neural network approaches, *Canadian Journal of Remote Sensing*, 20:396–407.
15. Piper, J., 1992, Variability and bias in experimentally measured classifier error rates. *Pattern Recognition Letters*, 13, 685–692.
16. Pohl, C., and J.L. van Genderen, 1998. Multisensor image fusion in remote sensing: Concepts, methods and applications, *International Journal of Remote Sensing*, 19(5):823–854.
17. Rao, R.M., and M.K. Arora, 2004. Overview of image processing, *Advanced Image Processing Techniques for Remotely Sensed Hyperspectral Data* (P.K. Varshney and M.K. Arora, editors), Springer-Verlag, 51–85.
18. Saha A. K., Arora M. K., Csaplovics E., Gupta R. P., 2005, Land Cover Classification Using IRS LISS III Image and DEM in a Rugged Terrain: A Case Study in Himalayas, *Geocarto International*, 20 (2): 39–46.
19. Sati, S.P., Sundriyal, Y.P., Rana, N., Dangwal, S., 2011. Recent landslides in Uttarakhand: nature's fury or human folly. *Curr. Sci.* 100 (11), 1617–1620.
20. Singh, R., Umrao, R.K., Singh, T.N., 2014. Stability evaluation of road-cut slopes in the Lesser Himalaya of Uttarakhand, India: conventional and numerical approaches. *Bull. Eng. Geol. Environ.* 73, 845–857.
21. Tso, B and Mather, P M. 200 1. *Classification Methods for Remotely Sensed Data*. Taylor and Francis, London, UK.
22. Simone, G., A. Farina, F.C. Morabito, S.B. Serpico, and L. Bruzzone, 2002. Image fusion techniques for remote sensing applications, *Information Fusion*, 3(1):3–15.
23. Watanachaturaporn, P., Arora, M.K. and Varshney, P.K., 2008. Multisource classification using support vector machines. *Photogrammetric Engineering & Remote Sensing*, 74(2), pp.239–246.
24. Wilkinson, G. G., 2000. Processing and classification of satellite images. *Encyclopaedia of Analytical Chemistry*, Edited by R. A. Meyers. John Wiley and sons, 8679–8693.
25. Yacouba, D., Guangdao, H. and Xingping, W., 2009. Assessment of land use cover changes using NDVI and DEM in Puer and Simao counties, Yunnan Province, China. *World rural observations*, 1(2), 1–11.
26. Zhu, A X. 1997. Measuring uncertainty in class assignment for natural resource maps under fuzzy logic. *Photogrammetric Engineering and Remote Sensing*, 63 (10), 1195–1202.